

Associative ionization in laser-excited sodium vapor

V. S. Kushawaha and J. J. Leventhal

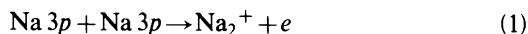
Department of Physics, University of Missouri-St. Louis, St. Louis, Missouri 63121

(Received 5 August 1981)

Associative ionization in Na $3s$ – Na $4d$ and Na $3s$ – Na $5s$ collisions has been studied using two dye lasers to produce excited sodium atoms. The rate constants for these processes are reported.

I. INTRODUCTION

Reactions involving excited sodium atoms have been the subject of several experimental studies in the last few years.¹⁻⁷ In most of these studies, atomic sodium was photoexcited with a laser beam tuned to a D line, and dimer ion formation in collisions between two Na $3p$ atoms was studied. In fact, this process, $3p$ – $3p$ associative ionization, has been shown to have a sufficiently high cross section^{4,6} so that the product electrons from



can act as seed electrons in a cascading process by which complete ionization¹ of a column of sodium vapor is achieved by irradiating it with D -line laser light. That is, the electrons from reaction (1) are superelastically heated in e -Na $3p$ collisions until they achieve enough kinetic energy to ionize the excited atoms.^{1,8,9} Each ionization adds another electron and an avalanche occurs.

Because $3p$ – $3p$ associative ionization proceeds fairly rapidly, it is also possible that other $nl/n'l'$ combinations, having energies comparable to that of two $3p$ sodium atoms, also lead to dimer ion formation. In particular, Koch *et al.*¹⁰ have suggested that their experiments, in which a plasma is produced by irradiating a heat pipe containing sodium vapor at $\sim 10^{17} \text{ cm}^{-3}$ with cw laser light tuned to either the $3p \rightarrow 4d$ (569 nm) or $3p \rightarrow 5s$ (616 nm) atomic transitions, can be explained if $3s$ – $4d$ and $3s$ – $5s$ associative ionization occurs. The radiation that they observe emanating from the heat pipe strongly suggests that a molecular ion plasma is produced and that associative ionization is an important step in the kinetic sequence of reactions leading to the plasma.

Because of the potential importance of associative ionization in these and other phenomena, we undertook a series of experiments to identify reactions of this type in laser excited sodium vapor,

and to measure the rate constants. In this paper we report the results of these experiments on $3s$ – $4d$ and $3s$ – $5s$ associative ionization.

II. EXPERIMENTAL

A schematic diagram of the apparatus is shown in Fig. 1. The collision cell is mounted on an oven and sodium vapor introduced through a slot in the bottom of the cell. Apertures in the cell permit laser beams to enter in opposite directions as shown; the apertures in the sides of the cell permit extraction of ions formed in the cell and observation of radiation.

For the experiments reported in this paper the output of a 6-W argon ion laser (Spectra Physics model 164-09) was split and used to pump two cw dye lasers (Spectra Physics Models 375 and 580A). The model 580A was operated at a single frequen-

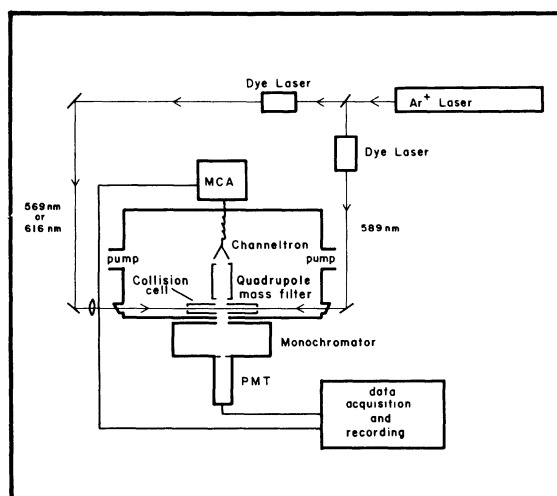


FIG. 1. Schematic diagram of the apparatus used in the present study.

cy with Rh-6G dye and tuned to the sodium D_2 line. The maximum output from this "yellow laser" was 16 mW which, at 498 K, excited about 7% of the sodium atoms lying within the cylinder defined by the beam (0.5-mm radius \times 2-cm long).

The second dye laser was operated multimode with either Rh-560 or Rh-6G dye (Exciton Chemical Company). With Rh-560, data were acquired with the wavelength tuned to the 569-nm $3p \rightarrow 4d$ atomic sodium transition; with Rh-6G the wavelength was set at the 616 nm $3p \rightarrow 5s$ atomic transition (Fig. 2). The maximum multimode output powers were 35 and 58 mW for green and red operation, respectively.

Photons emanating from the collision cell were dispersed and detected with a 0.25-m scanning monochromator and a cooled photomultiplier tube operated in the counting mode. Appropriate notch filters and neutral density filters were used to reduce fluorescence signals to avoid damage to the photomultiplier and to avoid tube saturation.

An electrostatic ion extraction lens and a quadrupole mass filter were located on the side of the cell opposite the optical system. Detection of the mass analyzed ions was accomplished with a channel particle multiplier also operated in the counting mode. For measurement of total ions, which was necessary for calculation of rate constants, the quadrupole mass filter was replaced by a total ion collector, and the ion current measured with an

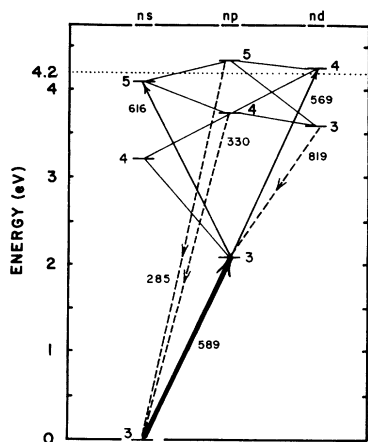


FIG. 2. Partial energy-level diagram of Na. The solid arrows represent transitions that are pumped by laser light and the dashed arrows are transitions observed in the experiment. The remaining lines represent allowed transitions not monitored in our present setup. The wavelengths of all transitions are in nanometers. The dotted line at 4.2 eV is the sum energy of two Na $3p$ atoms.

electrometer.

In these experiments the sodium atom density, $n(3s)$, was $\sim 10^{13} \text{ cm}^{-3}$, as determined by a method previously described⁶; this method employs both ion impact and surface ionization. The excited-state densities, $n(3p)$, $n(4d)$, and $n(5s)$, were determined by monitoring the 589, 569, and 616-nm fluorescence, respectively. This method of determining excited-state densities requires accurate calibration of the optical system which was achieved using an Optronic Model L-120 quartz halide lamp in conjunction with a series of narrow band filters to eliminate scattered light. The total fluorescence photon flux, ϕ , in photons per second, was determined using the relation

$$\phi = [I_s(\lambda)/E(\lambda)][4\pi/\langle\Omega(s)\rangle], \quad (2)$$

where $I_s(\lambda)$ is the observed photon count rate at wavelength λ , $E(\lambda)$ is the optical system efficiency at wavelength λ as determined with the calibrated lamp, and $\langle\Omega(s)\rangle$ is the average solid angle subtended by the slit. In this work all fluorescence data were obtained using 1000- μm slits for which the solid angle is smaller than that of the monochromator. Of course, the use of Eq. (2) carries the implicit assumption that the fluorescence is isotropically distributed in space. For determination of $n(3p)$ it was also necessary to measure the trapped lifetime of the $3p$ state.¹¹ In our previous publication,⁶ $n(3p)$ was determined from the value of $n(3s)$ and the presumed saturation of the $3s_{1/2} \rightarrow 3p_{3/2}$ transition. The present method indicates that the value thus obtained for $n(3p)$ was too high by about a factor of 2. A corrected value of the rate constant, deduced from these data, will be presented later in this paper. Table I is a listing of the atom densities at 498 K, the temperature at which most data were acquired. The temperature range accessible in these experiments was limited to 490–515 K.

TABLE I. Atom densities, $n(nl)$, at 498 K determined as described in the text.

nl	$n(nl)$ ($\text{cm}^{-3} \times 10^{-12}$)	Laser power (mW)
3s	19	
3p	1.2	16 ^a
4d	0.04	35 ^b
5s	0.2	58 ^b

^aSingle frequency.

^bMultimode.

III. RESULTS AND DISCUSSION

All experiments reported in this paper were performed with the yellow laser tuned to the sodium D_2 line which resulted in a small "background" Na_2^+ signal from $3p/3p$ associative ionization. The measured Na_2^+ signal from $3s/4d$ or $3s/5s$ collisions was corrected for this background. All Na_2^+ signals disappeared when the yellow laser was either detuned from the D line or was blocked completely.

When the green laser was tuned to the $3p \rightarrow 4d$ atomic transition and superimposed on the cell containing both Na $3s$ and Na $3p$ the yield of Na_2^+ increased dramatically. No Na^+ was observed indicating that the $3p/4d$ Penning ionization rate constant must be lower than $10^{-16} \text{ cm}^3/\text{sec}$. Figure 3 shows a log-log plot of both the 330-nm radiation signal and the Na_2^+ ion signal as functions of the laser power density of the green laser with wavelength set at the $3p \rightarrow 4d$ atomic transition. Although small yields of 330-nm radiation result from collisional processes, the major part of this signal is from cascading from Na $4d$. This signal is therefore proportional to the population of Na $4d$, although $n(4d)$ was determined as discussed in Sec. II of this paper. The unit slope of the straight line representing the 330-nm radiation versus laser power density in Fig. 3 shows that, as expected, formation of Na $4d$ requires only a single photon from the green laser. The unit slope of the straight line representing the Na_2^+ count rate

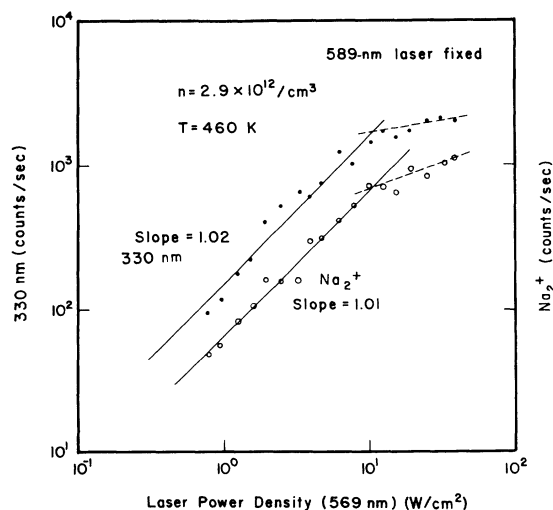


FIG. 3. Log-log plot of the 330-nm radiation and the Na_2^+ count rates vs the laser power density of the green (569-nm) laser at a fixed power density of the yellow (589-nm) laser.

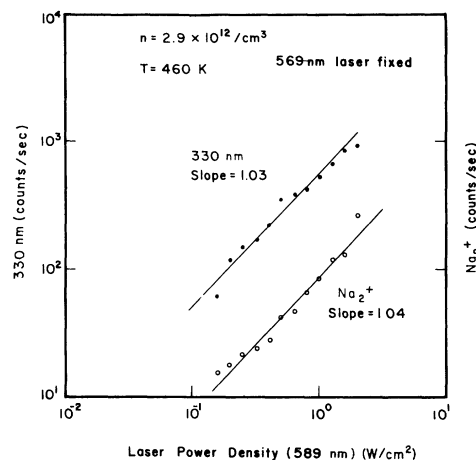


FIG. 4. Log-log plot of the 330-nm radiation and the Na_2^+ count rates vs the laser power density of the yellow (589-nm) laser at a fixed power density of the green (569-nm) laser.

versus laser power density confirms that only a single 569-nm photon, superimposed on the $3s - 3p$ mixture, is required to form Na_2^+ . It is interesting that both signals tend to constant values above $\sim 10 \text{ W/cm}^2$. Examination of the rate equations for photoexcitation of Na $3p$ and Na $4d$, and their subsequent decay shows that this effect is due to depletion of the $3p$ level.

It is energetically possible that the observed Na_2^+ ions could result from $3p - 4d$ collisions. If that were the case, then production of Na_2^+ would require two photons from the yellow laser beam; one to produce reactant Na $3p$ and the other for the first step in the $3s \rightarrow 3p \rightarrow 4d$ excitation that produces reactant Na $4d$. Thus, a log-log plot of the Na_2^+ signal as a function of yellow laser power density would yield a straight line with slope 2. Figure 4 shows these data. Also shown is the 330-nm fluorescence, as before indicative of the Na $4d$ population. The slope of the straight line for Na_2^+ is unity rather than 2, and establishes the source of Na_2^+ ion, with both yellow and green lasers irradiating the cell, as $3s - 4d$ associative ionization. This observation, together with the ab-

TABLE II. Rate constants for associative ionization.

Collision	Rate constant (cm^3/sec)
$3p/3p$	1.3×10^{-12}
$3s/4d$	7.8×10^{-11}
$3s/5s$	3.3×10^{-13}

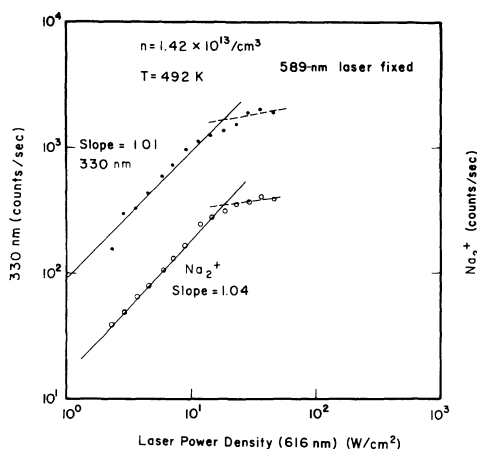


FIG. 5. Log-log plot of the 330-nm radiation and the Na₂⁺ count rates vs the laser power density of the red (616-nm) laser at a fixed power density of the yellow (589-nm) laser.

sence of any atomic ion signal from 3*p*–4*d* Penning ionization, indicates that 3*p*–4*d* collisions are relatively unimportant.

In order to calculate the rate constant for 3*s*–4*d* associative ionization the quadrupole mass filter was replaced by a total ion collector. The rate constant is given by

$$k_{\text{ion}} \left(\frac{3s}{4d} \right) = \frac{i_{\text{ion}}}{1.6 \times 10^{-19}} / \int n(3s)n(4d) dV, \quad (3)$$

where i_{ion} is the measured ion current. As described previously it was assumed that the densi-

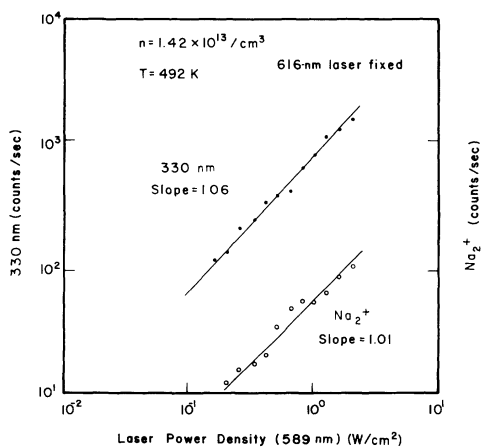


FIG. 6. Log-log plot of the 330-nm radiation and the Na₂⁺ count rates vs laser power density of the yellow (589-nm) laser at a fixed power density of the red (616-nm) laser.

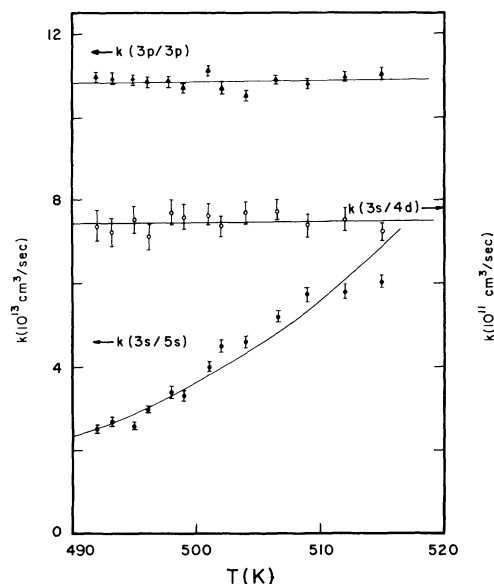


FIG. 7. Temperature dependence of the rate constants for associative ionization.

ty $n(4d)$ was constant over the cylinder defined by the laser beam so that the integral in Eq. (3) reduces to the product of the densities and the volume of that cylinder. The rate constant, $k_{\text{ion}}(3s/4d)$, determined in this way was found to be 7.8×10^{-11} cm³/sec at 498 K. This value is nearly 2 orders of magnitude greater than $k_{\text{ion}}(3p/3p)$, which we have measured to be 1.3×10^{-12} cm³/sec, and about a factor of 200 greater than that measured for $k_{\text{ion}}(3s/5s)$ in this work. The results are summarized in Table II. The value of $k(3p/3p)$ quoted above differs from that reported previously⁶ by us; this revision is due to the improved technique for measurement of

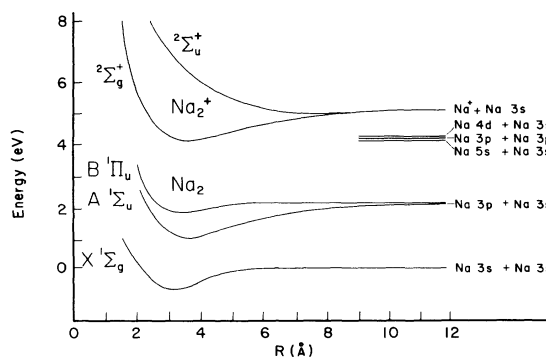


FIG. 8. Partial potential energy curves of Na₂ and Na₂⁺.

$n(3p)$ discussed in Sec. II of this paper. Both $k_{\text{ion}}(3p/3p)$ and $k_{\text{ion}}(3s/4d)$ were independent of temperature over the range 490–515 K.

The experimental procedure for study of $3s-5s$ associative ionization was identical to that employed to study the $3s-4d$ process except that the green (569-nm) laser was converted to a red (616-nm) laser tuned to the $3p \rightarrow 5s$ atomic sodium transition. Figures 5 and 6 are analogous to Figs. 3 and 4 and establish the necessity of a single 616-nm photon to produce Na_2^+ , and the absence of $3p-5s$ Penning ionization. (The rate constant for $3p/5s$ Penning ionization must be lower than 10^{-18} cm³/sec.) Unlike $3p-3p$ and $3s-4d$ associative ionization $k_{\text{ion}}(3s/5s)$ was observed to be temperature dependent. Figure 7 is a plot of the three rate constants as functions of temperature as determined in these experiments. An Arrhenius plot of $\ln[k_{\text{ion}}(3s/5s)]$ vs $1/T$ yields an activation energy of ~ 0.9 eV, nearly ten times the energy difference between the lowest vibrational level of the ground electronic state of Na_2^+ and the $\text{Na } 3s - \text{Na } 5s$

separated atom limit as shown in Fig. 8. While this seems to be an unusually large activation energy, given the thermochemical energy difference, the absence of detailed information on the $3s-5s$ potential energy curves makes it difficult to draw additional conclusions. For example, if one of the $3s-5s$ potential curves is repulsive to the extent that it intersects the ground electronic state of Na_2^+ at some high vibrational level, a high activation energy would result.

ACKNOWLEDGMENTS

This research was supported by the U. S. Department of Energy under Contract No. DE-AS02-76-ER02718. We would like to thank Mr. W. P. Garver for his help in acquiring lifetime data of $\text{Na } 3p$ and to M. R. Pierce and C. E. Burkhardt for initial calculations of the rate equations. We acknowledge the technical help of G. J. McClure and J. S. Mathews.

¹T. B. Lucatorto and T. J. McIlrath, Phys. Rev. Lett. **37**, 428 (1976).

²M. Allegrini, G. Alzetta, A. Kopystynska, L. Moi, and G. Orriols, Opt. Commun. **22**, 329 (1977).

³G. H. Bearman and J. J. Leventhal, Phys. Rev. Lett. **41**, 1227 (1978).

⁴A. de Jong and F. van der Valk, J. Phys. B **12**, L561 (1979).

⁵F. Roussel, P. Breger, G. Spiess, C. Manus, and S. Geltman, J. Phys. B **13**, L631 (1980).

⁶V. S. Kushawaha and J. J. Leventhal, Phys. Rev. A **22**,

2468 (1980).

⁷J. Weiner and P. Polak-Dingles, J. Chem. Phys. **74**, 508 (1981).

⁸R. M. Measures and P. T. Cardinal, Phys. Rev. A **23**, 804 (1981), and references cited therein.

⁹S. Geltman, J. Phys. B **10**, 3057 (1977).

¹⁰M. E. Koch, K. K. Verma, and W. C. Stwalley, J. Opt. Soc. Am. **70**, 627 (1977), and private communication.

¹¹W. P. Garver, Rev. Sci. Instrum. **52**, 607 (1981).